

# Evidence for Harmonic Content and Frequency Evolution of Oscillations during the Rising Phase of X-ray Bursts from 4U 1636–536

Sudip Bhattacharyya<sup>1,2</sup>, and Tod E. Strohmayer<sup>2</sup>

## ABSTRACT

We report on a study of the evolution of burst oscillation properties during the rising phase of X-ray bursts from 4U 1636–536 observed with the proportional counter array (PCA) on board the Rossi X-Ray Timing Explorer (RXTE). We present evidence for significant harmonic structure of burst oscillation pulses during the early rising phases of bursts. This is the first such detection in burst rise oscillations, and is very important for constraining neutron star structure parameters and the equation of state models of matter at the core of a neutron star. The detection of harmonic content only during the initial portions of the burst rise is consistent with the theoretical expectation that with time the thermonuclear burning region becomes larger, and hence the fundamental and harmonic amplitudes both diminish. We also find, for the first time from this source, strong evidence of oscillation frequency increase during the burst rise. The timing behavior of harmonic content, amplitude, and frequency of burst rise oscillations may be important in understanding the spreading of thermonuclear flames under the extreme physical conditions on neutron star surfaces.

*Subject headings:* equation of state — methods: data analysis — stars: neutron — X-rays: binaries — X-rays: bursts — X-rays: individual (4U 1636–536)

## 1. Introduction

Millisecond period brightness oscillations, “burst oscillations”, during thermonuclear (type I) X-ray bursts from the surfaces of neutron stars in low mass X-ray binary (LMXB) systems result from an asymmetric brightness pattern on the rotating stellar surface (Chakrabarty

---

<sup>1</sup>Department of Astronomy, University of Maryland at College Park, College Park, MD 20742-2421

<sup>2</sup>Laboratory for High Energy Astrophysics, Goddard Space Flight Center, NASA, Greenbelt, MD 20771; sudip@milkyway.gsfc.nasa.gov, stroh@clarence.gsfc.nasa.gov

et al. 2003; Strohmayer, & Bildsten 2003). This timing feature reveals the stellar spin period and can provide important information about the other stellar parameters (radius, mass, etc.; Miller, & Lamb 1998; Nath, Strohmayer, & Swank 2002; Muno, Özel, & Chakrabarty 2002). Theoretical modelling of these oscillations has the potential to constrain the equation of state (EOS) of the dense matter at the core of a neutron star (Bhattacharyya et al. 2005). This can be most effectively done if the burst oscillation has some harmonic content, as the fitting of a pure sinusoidal lightcurve does not put strong constraints on the stellar parameters. Although burst oscillations have been discovered from more than a dozen LMXBs, only one source (the accreting millisecond pulsar XTE J1814-338) has shown significant harmonic content (during burst decay; see Strohmayer et al. 2003; Watts, Strohmayer, & Markwardt 2005). In this Letter we focus on oscillations during burst rise, because at the beginning of the burst, the size of the burning region (hot spot) is theoretically expected to be at its smallest, and the harmonic content should theoretically be larger, and hence might be detected.

The study of burst oscillations during burst rise is important for another reason. At the onset of the burst, a small portion of the stellar surface is ignited, and then the burning region spreads and engulfs the whole stellar surface during the burst rise (Spitkovsky, Levin, & Ushomirsky 2002). This is natural, because simultaneous ignition of the whole stellar surface would require very fine tuning. Understanding this spreading is important, as it involves complex nuclear physics and geophysical fluid dynamics (with significant stellar spin), under conditions of extreme gravity, magnetic field and radiation pressure. Other than the burst rise lightcurve, the time evolution of three properties (frequency, amplitude, and harmonic content) of burst oscillations are the most useful observational tools to investigate this problem. Studies to date have not found harmonic content during burst rise. Strohmayer, Zhang, & Swank (1997) found evidence for a decrease in amplitude during burst rise from an analysis of RXTE data from the LMXB 4U 1728-34. Frequency increase during the burst rise from the accreting millisecond pulsar SAX J1808.4–3658 has also been reported (Chakrabarty et al. 2003).

In this Letter, we study burst oscillation properties of the LMXB 4U 1636–536 during burst rise. This is a regular bursting source and the Rossi X-ray Timing Explorer (RXTE) has discovered oscillations during many bursts from this source over the course of its mission. The oscillation frequency is  $\sim 582$  Hz. Here, we report the finding of frequency evolution during the rise of several bursts, as well as evidence for significant harmonic content of burst oscillations at the beginning of burst rise.

## 2. Data Analysis and results

More than a hundred bursts have so far been observed from the LMXB 4U 1636–536 by the proportional counter array (PCA) on board RXTE. By analysing the archival data we find that 23 of them show at least moderately strong oscillations during burst rise. In order to search sensitively for harmonic content, it is necessary to maximize the fundamental power by taking any frequency evolution into account (see Miller 1999; Strohmayer & Markwardt 1999; Muno et al. 2002). Therefore, first we explore frequency evolution during burst rise using the following procedures: (1) we calculate dynamic power spectra (Strohmayer & Markwardt 1999) using a time duration that is small enough to resolve the burst rise, but is still large enough to accumulate significant signal power. The resulting dynamic spectra (see for example, panel *a* of Fig. 1, and Fig. 2) provide an indication of the frequency evolution behavior. (2) We carry out a phase timing analysis (Muno et al. 2000) to confirm the indications in the dynamic spectra. We divide the burst rise time interval into several bins of a fixed chosen length, and then assuming a frequency evolution model, we calculate the average phase ( $\psi_k$ ) in each bin ( $k$ ). We use simple polynomial models to describe the frequency evolution. The corresponding  $\chi^2$  is calculated using the formula  $\chi^2 = \sum_{k=1}^M (\psi_k - \bar{\psi}_k)^2 / \sigma_{\psi_k}^2$  (Strohmayer & Markwardt 2002), where  $M$  is the number of bins, and  $\sigma_{\psi_k} = 1/\sqrt(Z_1^2)$  ( $Z_1^2$  is the fundamental power in the corresponding bin). We find the best fit parameter values for a particular frequency evolution model by minimizing this  $\chi^2$  and we calculate the uncertainty in each parameter by increasing the  $\chi^2$  value by the appropriate amount (Strohmayer & Markwardt 2002; Press et al. 1992). (3) To confirm these results, we calculate the total fundamental power ( $Z_1^2$ ) during the burst rise time interval using these best fit frequency evolution model parameter values, and ensure that this power is close to the maximum power obtained from any parameter values.

We discover four bursts with significant frequency evolution during the rise. These are listed in Table 1. Burst A shows the clearest evidence of frequency increase (see panel *a* of Fig. 1). For this burst, a constant frequency model gives a reduced  $\chi^2 = 195.03/6$  and fundamental power  $Z_1^2 = 57.41$ . We also calculated the phase residuals (see Strohmayer & Markwardt 2002 for details) for this model. The large systematic deviations from the mean value (panel *b* of Fig. 1), and the very high  $\chi^2$  indicate that a constant frequency model for burst A can be strongly rejected. Next, we add a linear term to the frequency model, and find that the corresponding reduced  $\chi^2 = 33.76/5$ , and  $Z_1^2 = 134.15$ . This is a better fit, but still not statistically acceptable. Therefore, we include a nonlinear term to the frequency model. This model has a reduced  $\chi^2 = 2.00/4$ , and  $Z_1^2 = 170.42$ , and the corresponding phase residuals have small random deviations from the mean value (panel *c* of Fig. 1). Hence, we conclude, that for burst A, the data strongly indicate a nonlinear frequency increase (Table 1).

We fit constant frequency models to the other bursts listed in Table 1. For bursts B, C, & D, the reduced  $\chi^2$  ( $Z_1^2$ ) values for this model are 225.58/6 (86.91), 43.84/6 (86.16), & 142.11/5 (20.42) respectively. These are all poor fits, and hence the constant frequency model for these bursts can be strongly rejected. Next, we include a linear term in the frequency models for these bursts. The corresponding reduced  $\chi^2$  ( $Z_1^2$ ) values are 7.16/5 (200.35), 12.70/5 (173.18), & 5.11/4 (89.75) respectively. These fits are acceptable for bursts B & D. For burst C, the high power value and the good visual fit of this frequency model to the power contours (panel *b* of Fig. 2) suggest that this model is on average correct, and the high reduced  $\chi^2$  value may be caused by fluctuation of the frequency on short time scales. Therefore, for bursts B, C, & D, a linear frequency increase (see Table 1) is highly probable.

In panel *d* of Fig. 1, we show the rms amplitude variation with time during the rise of burst A. The fundamental amplitude shows an initially fast and then a slower decrease. Moreover, there is some weak indication of a significant 1st harmonic amplitude during the first  $\sim 1/2$  second of this burst.

Using our best fitting frequency evolution models, we searched for harmonic content in the burst oscillations. Individually, none of the bursts shows strong harmonic power, therefore, we added the bursts coherently to get more signal. For this purpose, we chose the bursts with fundamental  $Z^2$  power  $> 30$  (for the constant frequency model) during burst rise, and added them (nine in number; mentioned in Table 2) coherently (i.e., we shifted the phases suitably in order to maximize the total fundamental power). The total co-added, phase-folded lightcurve does not give a significant harmonic power. A possible reason for this may be that during a significant portion of the burst rise interval, the size of the burning region is large enough that the harmonic amplitude is small and not detectable. To further address this possibility we consider five time intervals (starting at the time of burst onset) of length; 1/4th, 1/3rd, half, 2/3rd, and all of the rise time. For each interval fraction, and for each burst, we consider that fraction of the total rise time, fit it with our frequency evolution model to get best fit parameter values, and use these best fit values to calculate the phases. We do this for all the nine bursts and then add them coherently (separately for each interval fraction). We find that the interval comprising 1/3rd of the rise time gives the highest harmonic power (17.52). The search at the harmonic frequency in any independent subinterval is essentially a single trial search (see Miller 1999), so we can estimate the significance of this value using a  $\chi^2$  distribution with 2 degrees of freedom. This gives a single-trial probability of  $1.57 \times 10^{-4}$  to find a power as high by chance. We searched 5 intervals, but they are not all independent, so the number of trials is between 1 and 5. Using 5 to get a conservative, lower bound on the probability gives  $7.85 \times 10^{-4}$ , which is still a bit better than a  $3\sigma$  detection. As we increase the time interval, (that is, use more of the rise), the harmonic power decreases gradually, which is consistent with the expectation that

with time the burning region becomes larger, and hence the harmonic content diminishes. Due to the consistency with this theoretical expectation, and the better than  $3\sigma$  harmonic power for 1/3rd of the rise interval, we conclude that harmonic content in the burst rise oscillations has been marginally detected.

We extracted the corresponding (i.e., for 1/3rd of the rise time interval) phase-folded lightcurve from the data (after subtraction of the persistent emission) of the nine bursts. We fit it with two models: (1) a single sinusoid (the fundamental) around a constant level, and (2) two sinusoids (fundamental and 1st harmonic) around a constant level. The former one gives a reduced  $\chi^2$  value 26.26/13, while this value for the latter model is 8.33/11 (Table 2). These results support our finding that the addition of a 1st harmonic provides a better description of the data. Fig. 3 shows the data, the best fit model (model 2 of Table 2), and all the components of the model.

### 3. Discussion

In this Letter, we report two new observational results: (1) the first detection of frequency evolution (increase) of burst rise oscillations from 4U 1636–536, and (2) the first evidence for harmonic content of burst rise oscillations (from any source). These effects may be a direct result of thermonuclear flame propagation on the stellar surface (Bhattacharyya & Strohmayer 2005a; 2005b). For example, consider ignition of a burst off of the equator in the northern hemisphere. Initially the burning region is relatively small. Its size is constrained by Coriolis forces and is given by the Rossby adjuusment radius (Pedlosky 1987; Spitkovsky et al. 2002). This confined burning region can produce both a large fundamental and harmonic amplitude, more or less consistent with the observations. The frequency, when first observed, is at its lowest value and then increases monotonically. At least two effects can account for this behavior; hydrostatic expansion—and subsequent spin-down—makes the burning region slip westward (on a star rotating eastward; see Strohmayer, Jahoda, Giles, & Lee 1997; Cumming & Bildsten 2001; Cumming et al. 2002; Spitkovsky et al. 2002; Bhattacharyya & Strohmayer 2005b), and the southbound front will slip even further westward due to conservation of angular momentum (Bhattacharyya & Strohmayer 2005b). Thus, the hot region initially has a net retrograde drift in the frame of the neutron star, so the observed frequency is less than the spin frequency. As the front approaches the equator it spreads faster, eventually forming a more or less symmetric equatorial belt (Spitkovsky et al. 2002). This can plausibly reduce the pulsation amplitude in both the fundamental and harmonic, and the westward drift slows because mass elements moving southward below the equator now drift eastward, conserving angular momentum. Thus, the frequency increases

from its initial (low) value. Once the equatorial belt has been ignited, it seems likely that residual asymmetry associated with the initial, northbound burning front is responsible for the observed, lower amplitude oscillations. Detailed calculations of the flux from such a spreading burning front are required to explore this scenario quantitatively, but the discussion above provides a plausible qualitative understanding of many of the observed properties (more detailed discussions are in Bhattacharyya & Strohmayer 2005b).

As noted above, the harmonic content found at the beginning of the bursts is consistent with the expected small size of the burning region. Although in this study we do not fit the phase-folded lightcurve (solid curve in Fig. 3) with realistic theoretical model lightcurves (such fitting may not be so straightforward to interpret, as the burning region geometries for bursts may be different), we have computed theoretical models to show that the inferred harmonic content is theoretically possible. For example, the harmonic to fundamental amplitude ratio ( $a_2/a_1$ ), and the relative phase difference ( $\epsilon_1 - \epsilon_2$ ) of the components can be reproduced reasonably well with a model assuming emission from a circular hot spot (Bhattacharyya et al. 2005). Using a dimensionless stellar radius-to-mass ratio  $Rc^2/GM = 4.5$ , stellar mass  $M = 1.5M_\odot$ , observer’s inclination angle  $i = 70^\circ$ ,  $\theta$ -position of the center of the circular burning region  $\theta_c = 50^\circ$ , angular radius of the burning region  $\Delta\theta = 25^\circ$ , beaming parameter  $n = 1.0$ , and blackbody temperature of the burning region  $T_{\text{BB}} = 2.0$  keV, we can explain the relative strength and phasing of the fundamental and harmonic components. Here, we have assumed a Schwarzschild spacetime, and the beaming parameter  $n$  gives a measure of the beaming in the frame corotating with the star (see Bhattacharyya et al. 2005 for a more detailed discussion of the model parameters). For the lightcurve calculated with these model parameter values, we find  $a_2/a_1 = 0.24$  and  $\epsilon_1 - \epsilon_2 = 0.41$ , while for the data (Fig. 3),  $a_2/a_1 = 0.24 \pm 0.06$  and  $\epsilon_1 - \epsilon_2 = 0.36 \pm 0.02$ . The constant level, required by the observed lightcurve, can plausibly be supplied by a symmetric belt-like component of the burning region (as mentioned earlier).

Although we have found reasonably strong evidence for harmonic structure at the onset of bursts, it required the addition of a significant number of bursts to increase the signal to noise ratio. These results suggest that detailed studies of the onset of bursts can, in principle, provide insight into the structure of neutron stars, and how thermonuclear flames propagate on their surfaces. Unfortunately, current studies are observationally limited by the detected count rates. For a larger count rate, the observed oscillation power in a given time interval would be greater. This would facilitate the detection of harmonic content, and also enable us to do more detailed studies of frequency and amplitude evolution. Therefore, new openings in this field are very likely with future larger area detectors.

This work was supported in part by NASA Guest Investigator grants.

## REFERENCES

Bhattacharyya, S., & Strohmayer, T. E. 2005a, submitted to ApJ.

Bhattacharyya, S., & Strohmayer, T. E. 2005b, in preparation.

Bhattacharyya, S., Strohmayer, T. E., Miller, M. C., & Markwardt, C. B. 2005, ApJ, 619, 483.

Chakrabarty, D. et al. 2003, Nature, 424, 42.

Cumming, A., & Bildsten, L. 2001, ApJ, 559, L127.

Cumming, A., Morsink, S. M., Bildsten, L., Friedman, J. L., & Holz, D. E. 2002, ApJ, 564, 343.

Miller, M. C. 1999, ApJ, 515, L77.

Miller, M. C. & Lamb, F. K. 1998, ApJ, 499, L37.

Muno, M. P., Fox, D. W., Morgan, E. H., & Bildsten, L. 2000, ApJ, 542, 1016.

Muno, M. P., Özel, F., & Chakrabarty, D. 2002, ApJ, 581, 550.

Nath, N. R., Strohmayer, T. E., & Swank, J. H. 2002, ApJ, 564, 353.

Pedlosky, J. 1987, *Geophysical Fluid Dynamics* (New York: Springer).

Press, W. H., Teukolsky, S. A., Vetterling, W. T., & Flannery, B. P. 1992, *Numerical Recepies in FORTRAN* (New York: Cambridge University Press), 687-693.

Spitkovsky, A., Levin, Y. & Ushomirsky, G. 2002, ApJ, 566, 1018.

Strohmayer, T.E., & Bildsten, L. 2003, in *Compact Stellar X-ray Sources*, Eds. W.H.G. Lewin and M. van der Klis, (Cambridge University Press: Cambridge), (astro-ph/0301544).

Strohmayer, T.E., Jahoda, K., Giles, A. B., & Lee, U. 1997, ApJ, 486, 355.

Strohmayer, T. E., & Markwardt, C. B. 1999, ApJ, 516, L81.

Strohmayer, T. E., & Markwardt, C. B. 2002, ApJ, 577, 337.

Strohmayer, T. E., Markwardt, C.B., Swank, J. H., & in 't Zand, J. 2003, ApJ, 596, L67.

Strohmayer, T. E., Zhang, W., & Swank, J. H. 1997, ApJ, 487, L77.

Watts, A. L., Strohmayer, T. E., & Markwardt, C. B. 2005, ApJ, in press (astro-ph/0508148).

Table 1. Frequency evolution model parameters<sup>a</sup>(with  $1\sigma$  error) for four bursts.

| ObsId          | Start date  | Burst | $\nu_0$                  | $\dot{\nu}$            | $\ddot{\nu}$            | $\chi^2$ | $Z_1^{2b}$ |
|----------------|-------------|-------|--------------------------|------------------------|-------------------------|----------|------------|
| 60032-05-03-00 | 2002 Jan 12 | A     | $577.70^{+0.24}_{-0.25}$ | $2.38^{+0.24}_{-0.25}$ | $-0.42^{+0.07}_{-0.07}$ | 2.00     | 170.42     |
| 60032-05-03-00 | 2002 Jan 13 | B     | $579.19^{+0.07}_{-0.07}$ | $0.81^{+0.06}_{-0.05}$ | –                       | 7.16     | 200.35     |
| 60032-05-05-00 | 2002 Jan 14 | C     | $580.62^{+0.12}_{-0.12}$ | $0.28^{+0.08}_{-0.08}$ | –                       | 12.70    | 173.18     |
| 60032-05-10-00 | 2002 Jan 22 | D     | $578.44^{+0.12}_{-0.13}$ | $1.21^{+0.11}_{-0.10}$ | –                       | 5.11     | 89.75      |

<sup>a</sup>Frequency evolution model:  $\nu(t) = \nu_0 + \dot{\nu}t + \ddot{\nu}t^2$ , where  $\nu_0 = \nu(0)$ .

<sup>b</sup>Fundamental power during burst rise.

Table 2. Fitting of phase-folded lightcurve<sup>a</sup> best fit parameter<sup>b</sup>values (with  $1\sigma$  error).

| Model          | $a_0$              | $a_1$              | $\epsilon_1$    | $a_2$             | $\epsilon_2$    | $\chi^2/\text{dof}$ |
|----------------|--------------------|--------------------|-----------------|-------------------|-----------------|---------------------|
| 1 <sup>c</sup> | $667.87 \pm 10.00$ | $241.42 \pm 14.23$ | $0.37 \pm 0.01$ | –                 | –               | 26.26/13            |
| 2 <sup>d</sup> | $668.99 \pm 10.00$ | $245.60 \pm 14.26$ | $0.37 \pm 0.01$ | $59.49 \pm 14.05$ | $0.01 \pm 0.02$ | 8.33/11             |

<sup>a</sup>Combination (for first 1/3rd of the rise time interval) of nine bursts from the following ObsIds (start date): 30053-02-02-02 (1998 Aug 19), 30053-02-02-00 (1998 Aug 20), 40028-01-02-00 (1999 Feb 27), 40028-01-08-00 (1999 Jun 18), 50030-02-01-00 (2000 Nov 05), 60032-05-03-00 (2002 Jan 12), 60032-05-03-00 (2002 Jan 13), 60032-05-05-00 (2002 Jan 14) and 60032-05-13-00 (2002 Feb 05).

<sup>b</sup>Model lightcurve intensity is  $I = a_0 + a_1 \sin(2\pi(\epsilon - \epsilon_1)) + a_2 \sin(4\pi(\epsilon - \epsilon_2))$ , where  $\epsilon$  is the phase variable.

<sup>c</sup>Only fundamental.

<sup>d</sup>Fundamental + 1st harmonic.

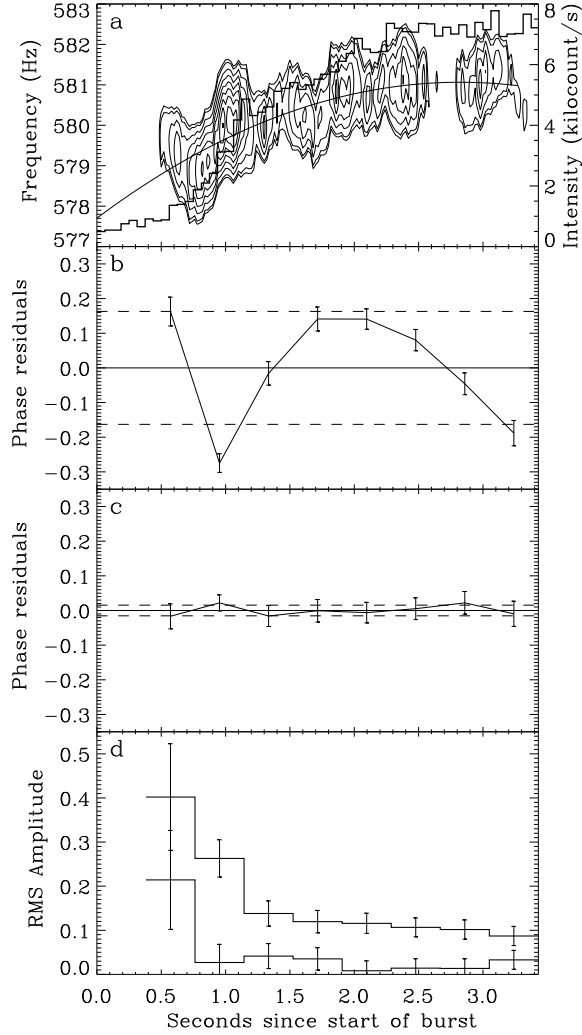


Fig. 1.— Time evolution of different observed burst properties during the rise of burst A (see Table 1) from 4U 1636–536. Panel *a* gives the detected intensity (histogram), power contours (minimum and maximum power values are 18 and 55) using dynamic power spectra (for 0.4 s duration at 0.02 s intervals), and the best fit model from Table 1. Panel *b* gives the phase residuals (phase varies from 0 to 1) and rms deviation (broken horizontal lines) for constant frequency (580.72 Hz) fitting. Panel *c* is same as panel *b*, but for the best fit values of frequency evolution parameters (Table 1). Panel *d* gives the rms amplitudes of brightness oscillation (persistent emission subtracted). The upper histogram is for the fundamental amplitude, and the lower histogram is for the 1st harmonic amplitude. Here the horizontal lines give the binsize and the vertical lines give  $1\sigma$  error.

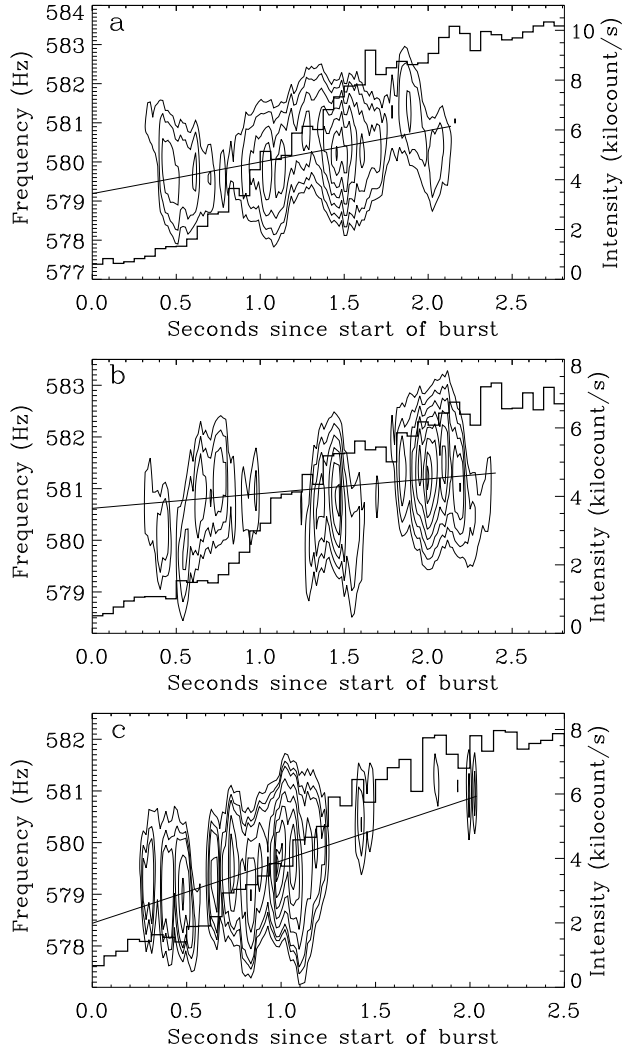


Fig. 2.— Similar as panel *a* of Fig. 1 (panel *a* is for burst B, panel *b* is for burst C, and panel *c* is for burst D). For each of the panels, the dynamic power spectra are calculated for 0.3 s duration at 0.015 s intervals. The minimum and maximum power values of the contours are (23, 77), (20, 53), and (15, 46) for panels *a*, *b*, and *c* respectively.

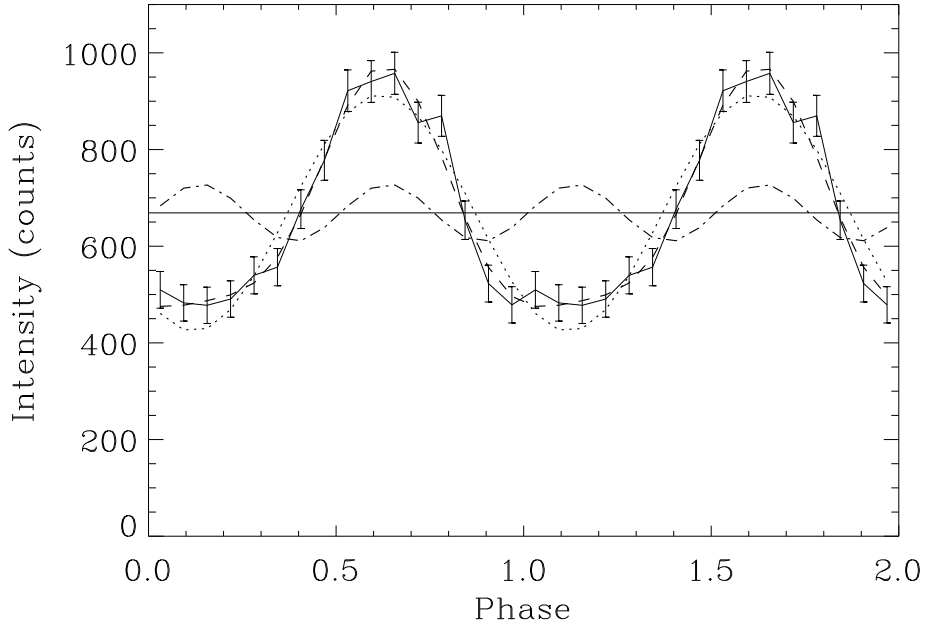


Fig. 3.— Phase-folded lightcurve of burst oscillation during burst rise from 4U 1636–536. The solid curve shows the data (combined for nine bursts for 1/3rd of the rise time interval; see Table 2), dashed curve is model 2 (see Table 2), solid horizontal line is the constant level of the model, dotted curve is the fundamental component of the model, and dash-dot curve is the 1st harmonic component of the model.